Spectral studies of the interstellar dust and CMB mm emission

F.-Xavier Désert (IPAG)

CMB-France Nov 2021

Abstract

We advocate R&D in spectroscopy with KIDs to tackle polarized foregrounds in the next generation CMB instruments. In particular, in order to remove the dust polarized emission, the use of low resolution spectrocopy may be required. I will present Grenoble efforts towards that goal, within the context of a nascent GIS.

Going to the submillimetre

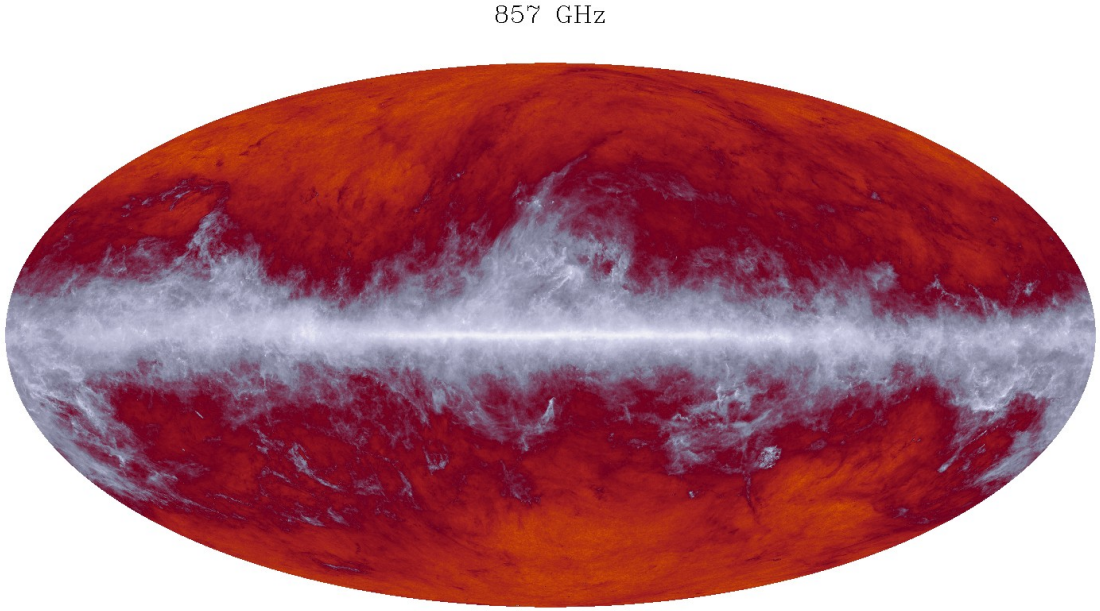

Planck 2015

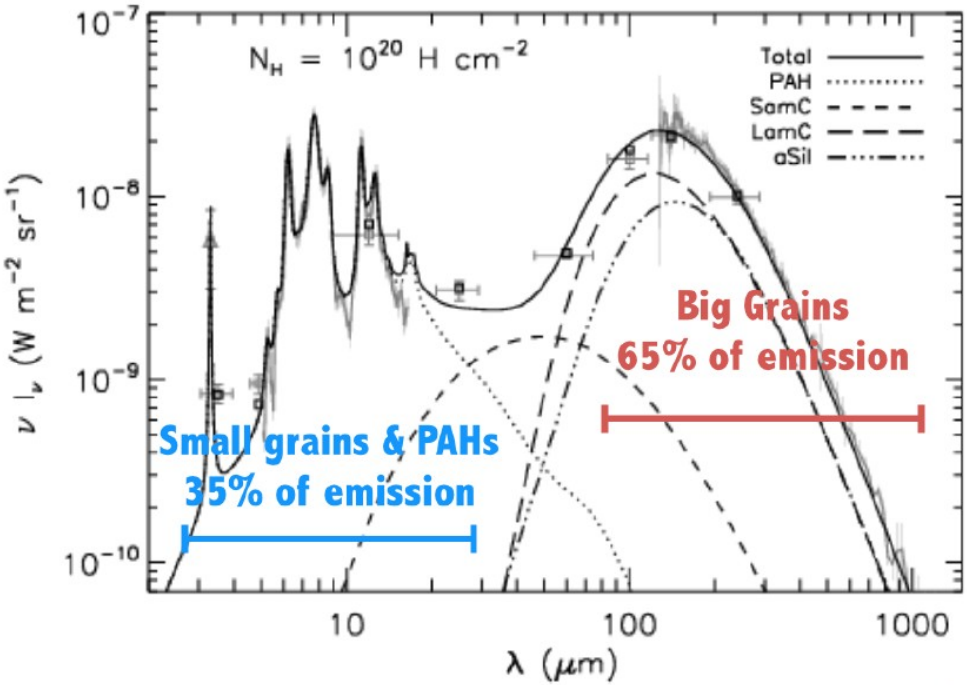

(Compiegne+2011)

Context

While the thermal dust component is modelled as a modified blackbody with free spectral index, βd, and temperature, Td. Planck 2018

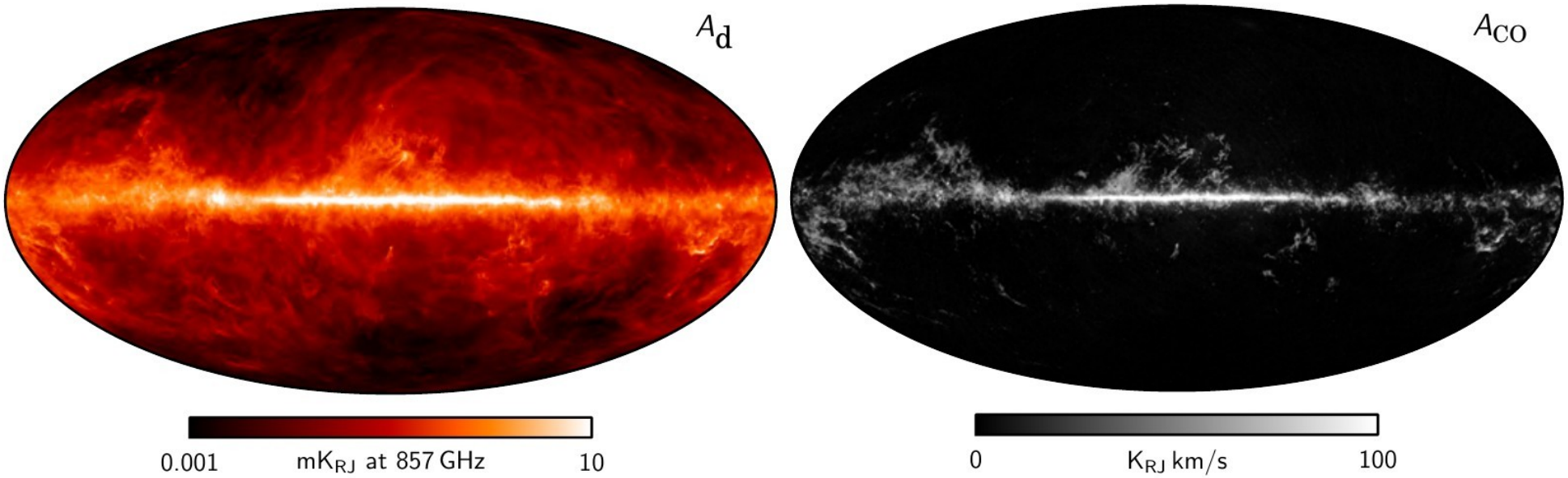

Fig. F.1. `Commander` foreground amplitude maps, derived from the *Planck* 2018 data set in intensity. *Top-left panel*: combined low-frequency foreground map at 40′ FWHM resolution, evaluated at 30 GHz, and accounts for synchrotron, free-free, and anomalous microwave emission. *Top-right panel*: derived radio point source map, as observed in the 30 GHz frequency channel. *Bottom-left panel*: thermal dust emission at 10′ FWHM resolution, evaluated at 857 GHz. Neither the CIB nor high-frequency point sources are fitted explicitly in the `Commander` 2018 temperature model, and these are therefore in effect included in this thermal dust emission map. *Bottom-right panel*: CO line-emission map, evaluated for the 100 GHz channel.

Beta-Td modified blackbody

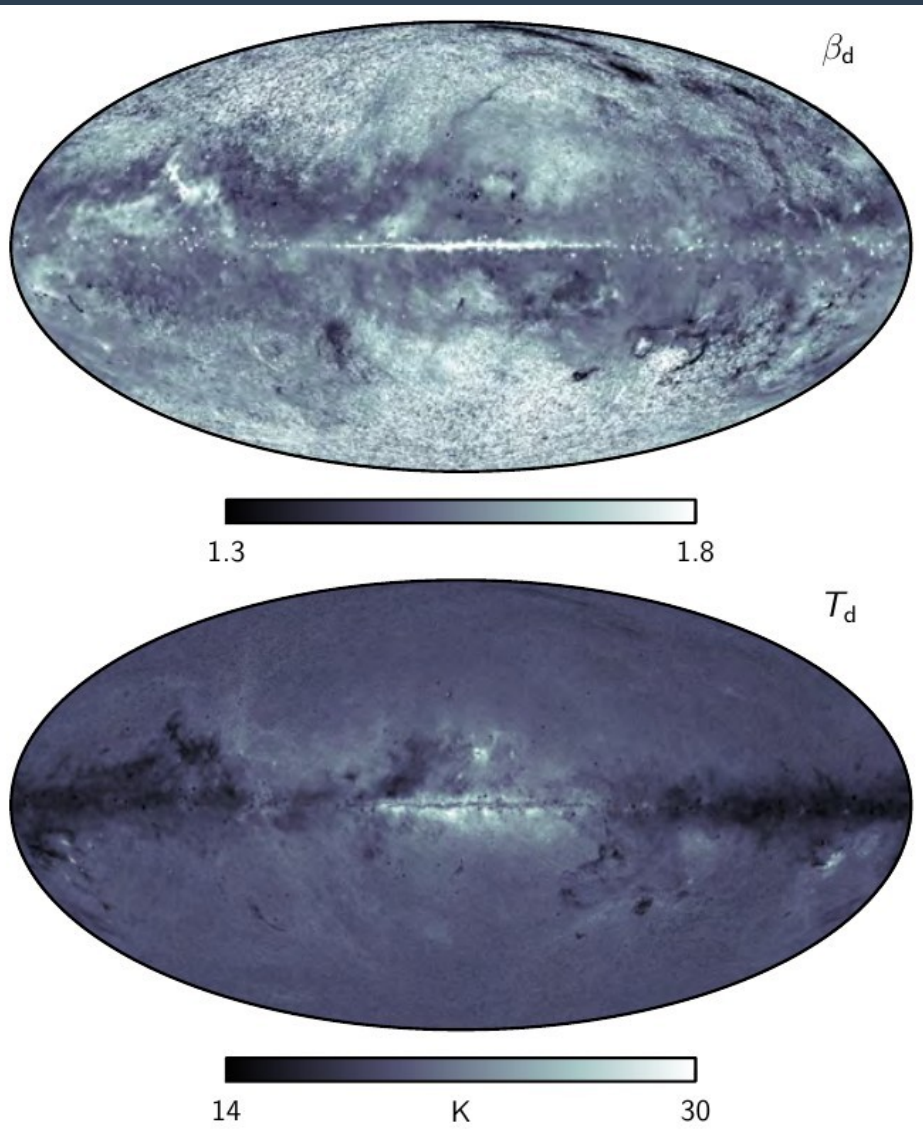

Fig. F.3. Commander 2018 foreground spectral parameters. *From top to bottom rows*: low-frequency spectral index at a 40′ FWHM smoothing scale, thermal dust spectral index at 10′ FWHM, and thermal dust temperature at 5′ FWHM, respectively.

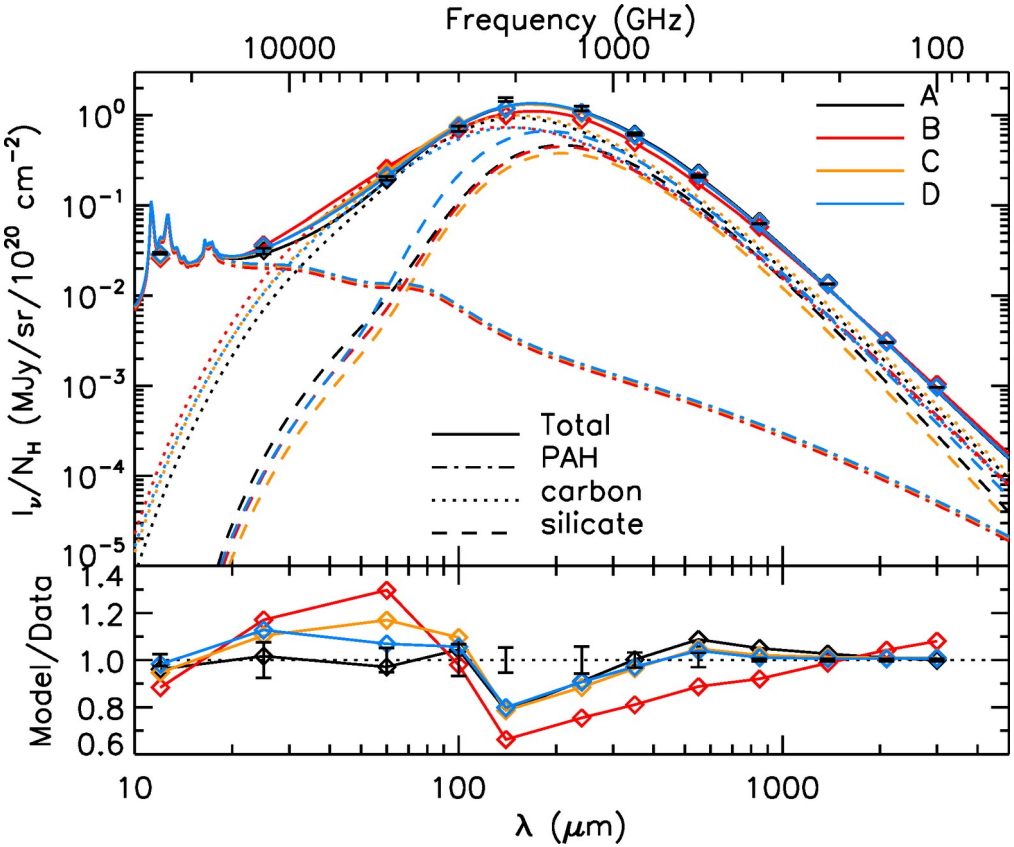

Guillet et al. 2018, AA610, A16

Central Molecular Zone
Herschel & Astec/LMT 1.1mm
Tang et al (2020)

- β increases towards denser regions of the Galactic center. Td decreases. Not due to degeneracy.
- β can be as large as 2.4!
- No model can explain that in a quantitative way (nor dust growth nor TLS, Meny et al 2007, Paradis et al. 2014)
- Uncertainty in temperature from assumed β at λ<500μm

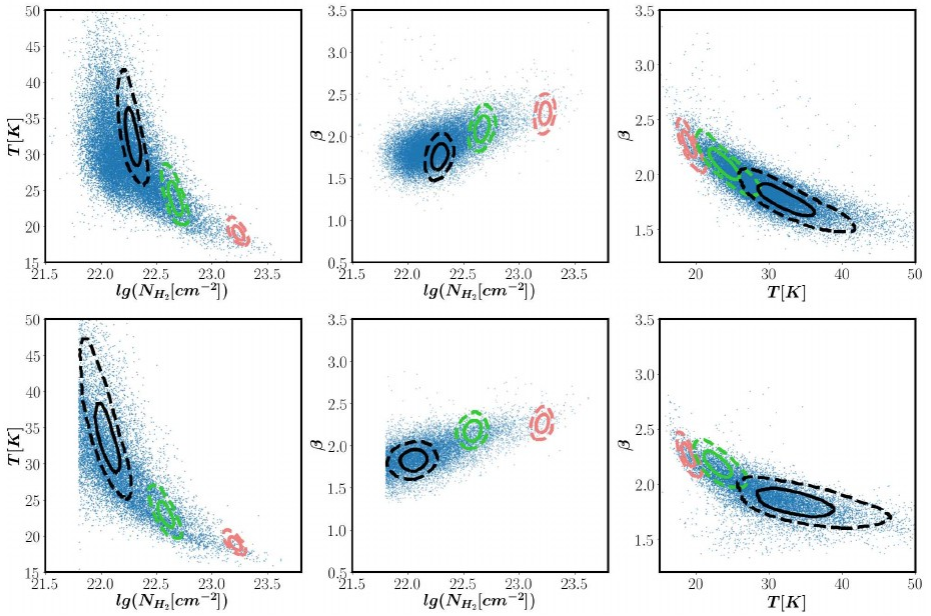

Figure 7. Upper panels: Correlations between parameters derived from the best-fit STMB model. Only the low Galactic latitude ($-0.2^\circ < b < 0.1^\circ$) cells (blue dots) are used in this derivation. Also plotted are the 1 and 3 σ confidence contours of three typical sampled posteriors at different representative locations in the parameter space. Lower panels: Similar plots after the fore/background subtraction, using only cells with $N_{H_2,cmz} > 10^{21.8}$.

Central Molecular Zone

- GASTON NIKA2 Large Program will shed light on these issues at 1-2 mm.
- Csengeri et al., 2016, Fusion of Laboca+Planck; see also Juvela et al : two-β model is necessary if mm data included

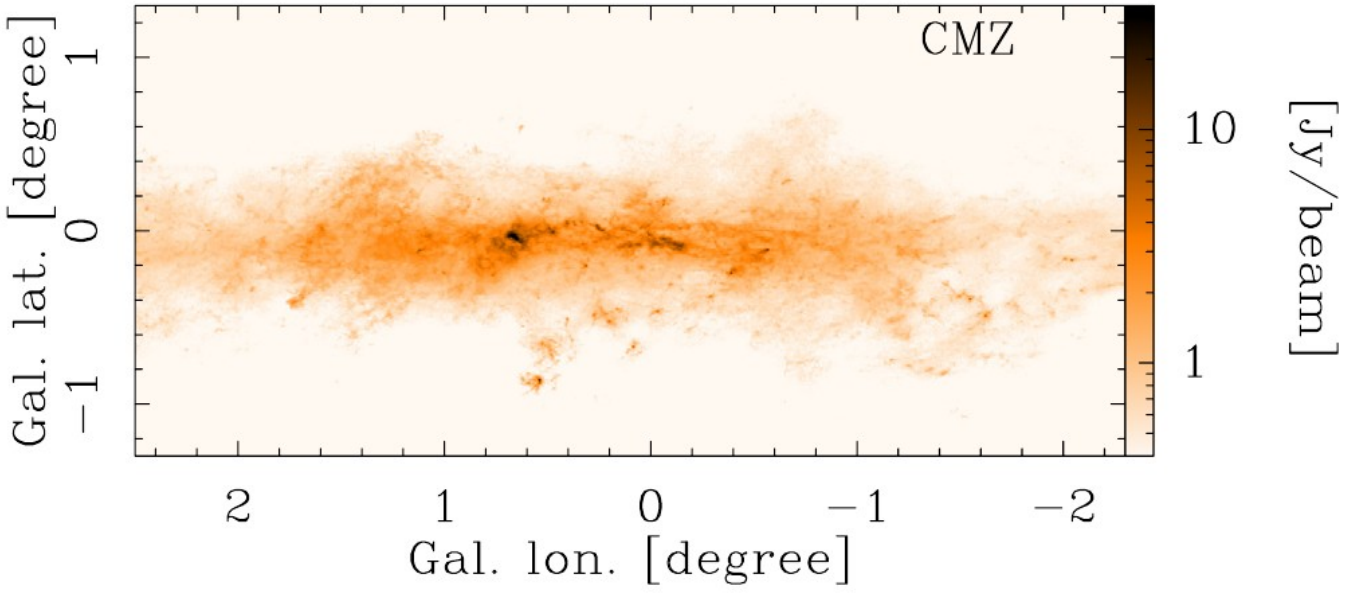

Nearby Galaxies

NGC1512,
Galametz et al., 2014, Laboca
Galliano et al, 2018, ARAA, 56, 673

NIKA2 Large Program on-going on Nearby galaxies,
PI: S. Madden

Observed

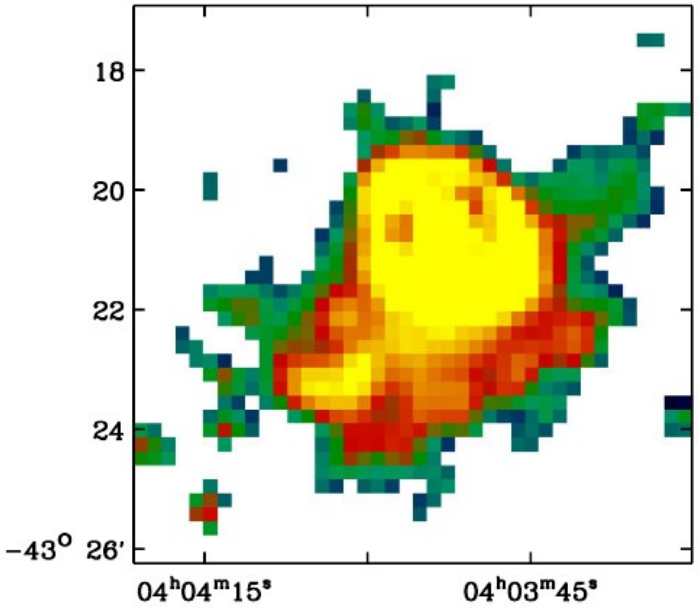

$\beta_c = 1.5$ model
Predicted from Herschel

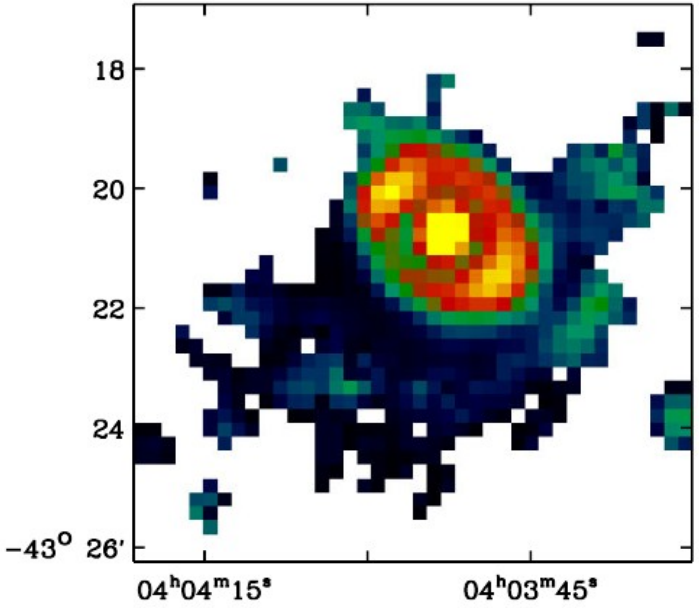

beta=1.5, 20K dust, introducing temperature spread (red)

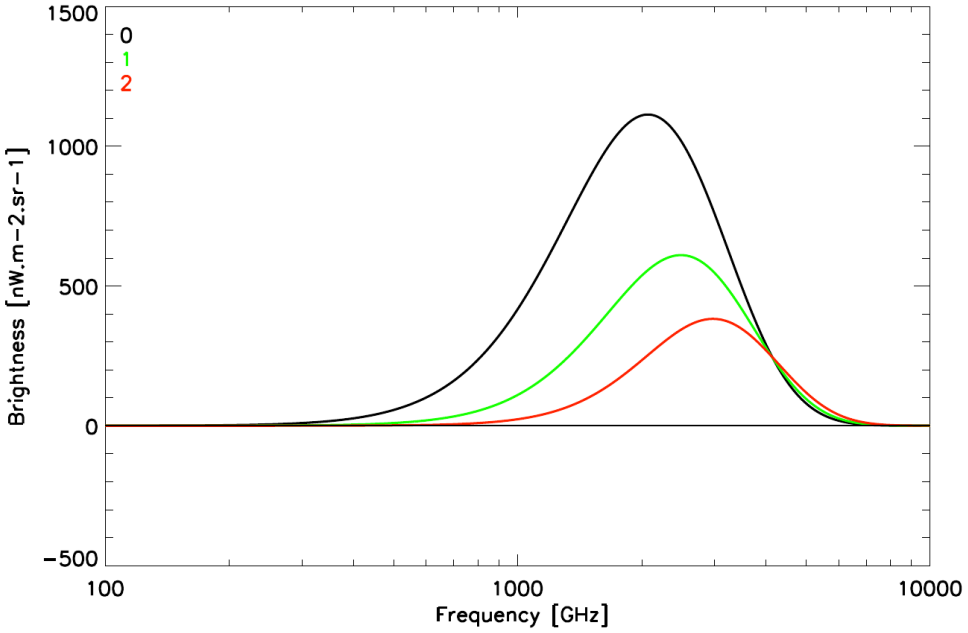

Multi-component approach

- Going beyond the greybody single temperature approach. Désert 2021 (arXiv, 2111.05046) following Pitrou&Stebbins 2014, and Chluba et al. 2017
- Importance of the map zero-levels. Recent improvements done by Delouis, Puget, Vibert, 2021, A&A, 650, A82 : Dust model goes towards beta angular variations, see also Mangilli et al. 2021.

Current issues in dust submillimetre emission

- Many component at mm: CO lines, free-free, synchrotron, and submm: several dust temperatures, dust constituents
- Models+experiments make predictions (Hensley&Draine 2021, ApJ906, 73; Demyk et al. 2017, AA, 606, A50) but ...
- CMB anisotropies and polarization (mm dust emission spectrum must be accurately known) e.g. Remazeilles et al. 2016, MNRAS, 458, 2032 show that 4 sigma bias can happen on *r* if wrong dust assumption. But so far Planck Coll 2020, AA, 641, A11 show encouraging news for future missions
- Need for spectral observations and parsimonious fitting method (Marsh et al. 2015, Chluba et al. 2017, Désert 2021).
- PRISM proposal contained 32 bands from 30 to 6000 GHz. PICO has 21 bands (21 to 709 GHz).
- ESA Voyage 2050 has a L mission with precision spectrocopic capabilities in the mm range (early Universe, z>8) and a medium mission for high resolution and/or intensity mapping.
- Concerto/APEX (next 2 slides)
- R&D, within the GIS Kids
- NIKA2 upgrade: low resolution spectral-pol. mapper
- CCat/FYST (6m), AtLAST (50m), Litebird(<1m), ...
- New telescope 15m (next FXD talk)?

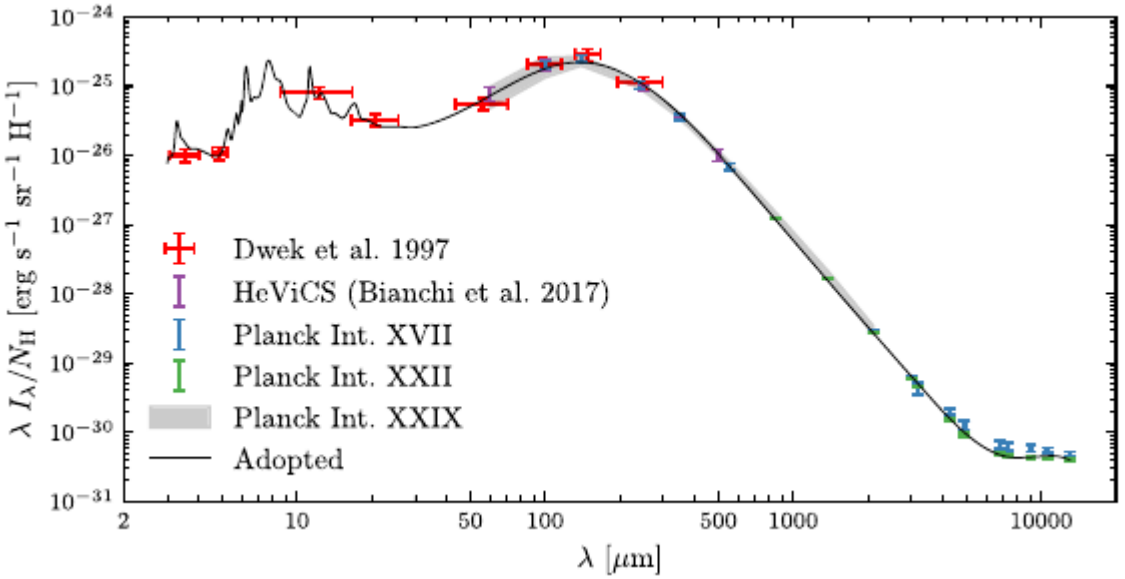

Concerto in a nutshell

- MPI, Fourier-Transform Spectrometer
- APEX 12m (5100m)@Chajnantor (MPIfR/ESO/OSO/Chile)
- ERC grant (P.I. G. Lagache). Commissionned Spring 2021, now taking science data (Early C+ intensity mapping of Cosmos field)
- 4300 Kids@100mK, 120-360GHz, sampled at 3.7 kHz
- MPI at 2.5 Hz gives resolution of up to 1.2 GHz (R up to 300)
- FOV=20 arcmin diameter, 5 MJy/sr. $s^{1/2}$@200GHz

Concerto coll. 2020

Courtesy:
A. Beelen

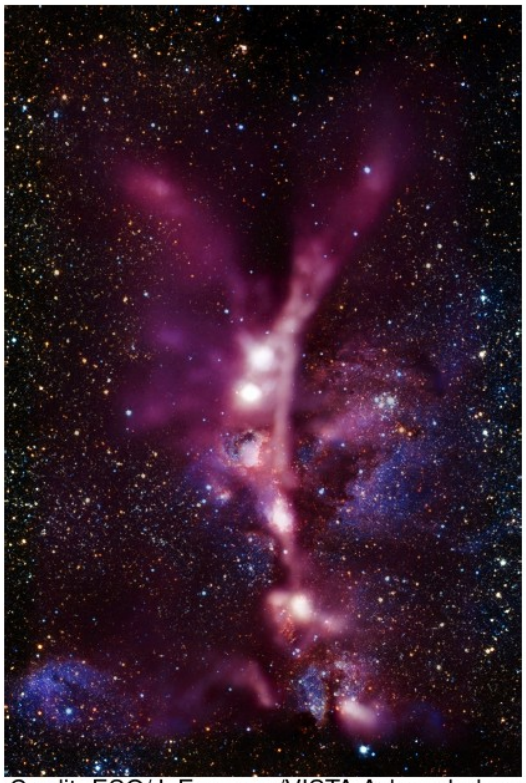

Credit: ESO/J. Emerson/VISTA Acknowledgment: Cambridge Astronomical Survey Unit

ESO Annoncement 21010 – 6th of July 2021

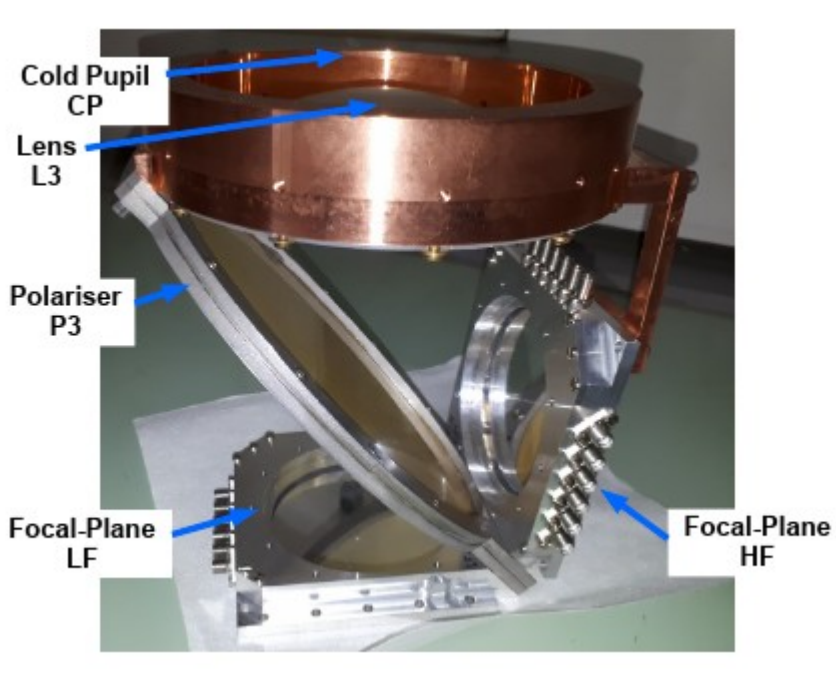

Concerto proposal

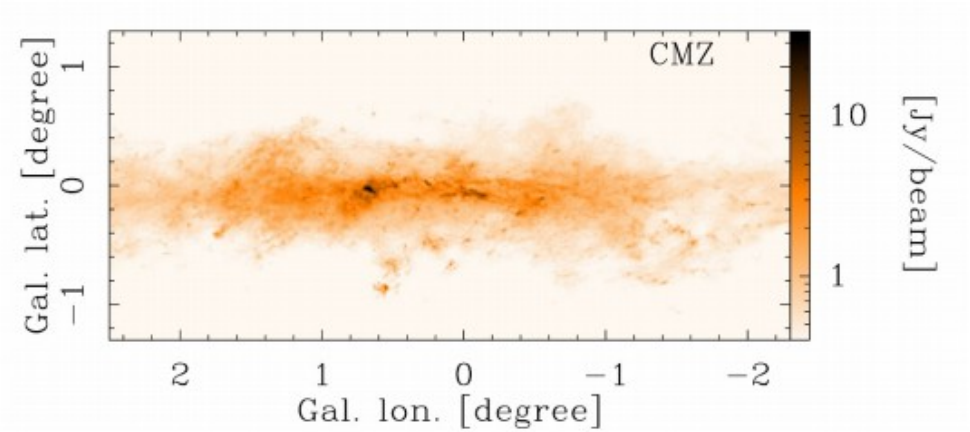

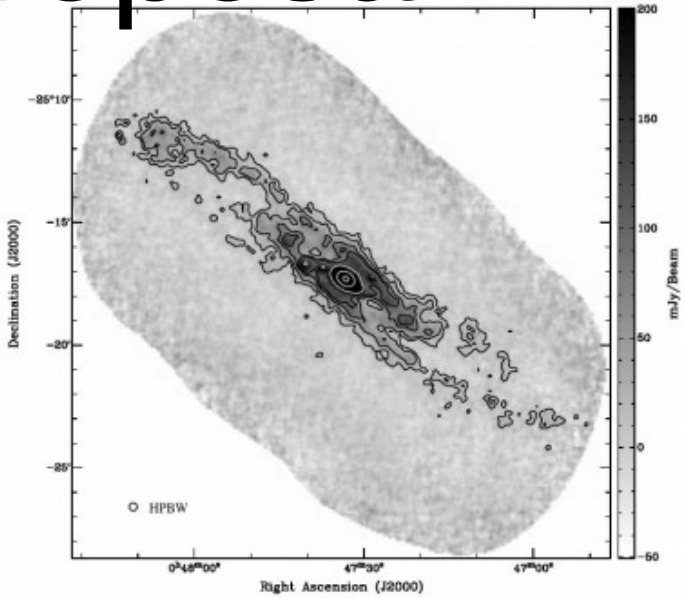

NGC253 (Laboca)
Weiβ et al 2008

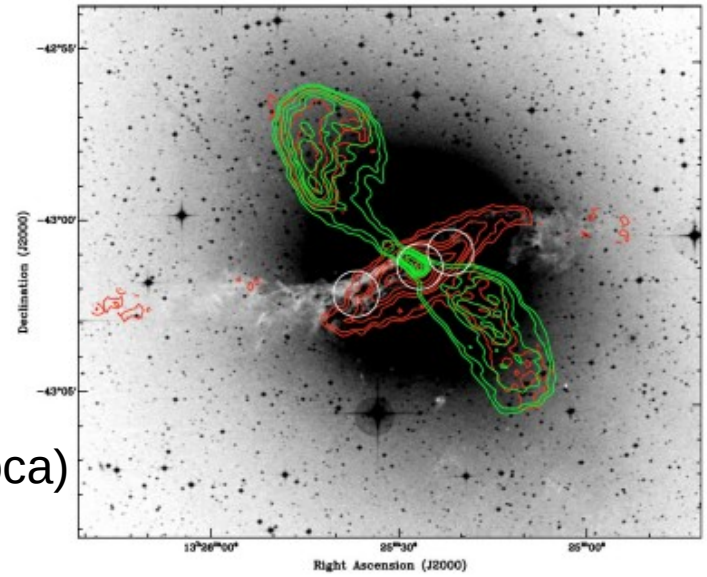

CenA (Laboca)

Observe reference galactic and extragalactic regions: map the dust spectral index with a spectro mapper for the first time

R&D low resolution spectroscopy 1/2

- Capitalize on our knowledge of KID technology
- Use previous experiences: spectro on chip (A. Monfardini), Fabry-Perot Interferometer (S. Bounissou's thesis), Spoc/Swifts concept (E. Le Coarer)
- no moving part, spectral capabilities close to the detectors
- enable polarization
- R=100-300
- Exchanges on-going within FOCUS labex (Grenoble-CEA)
- Need money! (ERC proposal)

R&D 2/2

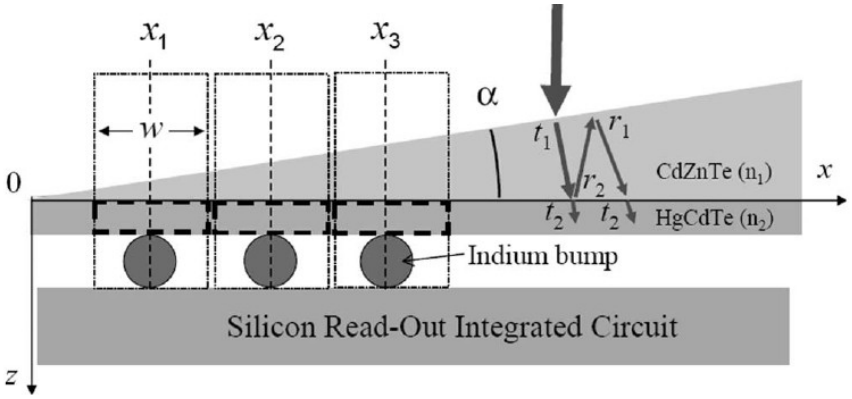

Fig. 1. Schematic view of a FTIR-FPA of HgCdTe technology.

Rommeluère et al. (2008)

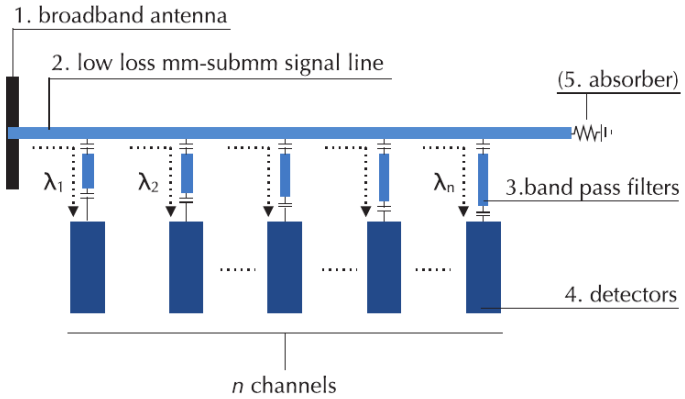

Fig. 1 Schematic diagram of an on-chip filterbank spectrometer for mm-submm waves. The signal enters the circuit from a broad band antenna (1). Then the signal is carried along a transmission line (e.g., microstrip line, coplanar waveguide) (2). From this signal line, multiple frequency channels branch out. Each channel consists of a narrow band pass filter (3) and a detector (4). The signal that is not absorbed in any of the channels gets absorbed at the end of the signal line, typically with a lossy piece of transmission line (5).

Endo (2015)

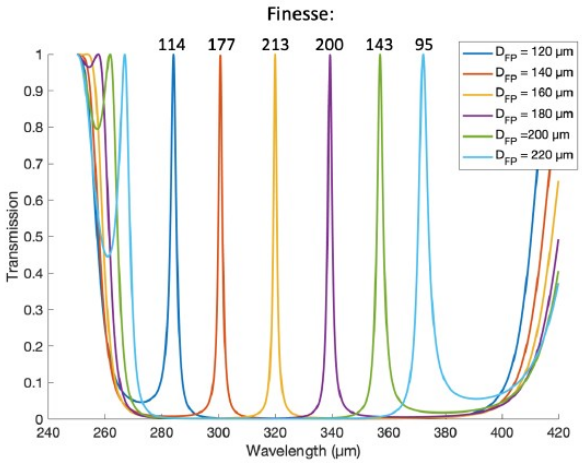

FIGURE 4.22: Computed transmission of the FPI presented in figure 4.20 for different cavity sizes of the FP D_{FP}. The finesse of each transmission peak has been computed and added on the plot above each peak : as expected the finesse is the highest for the wavelength that the mirrors geometry is adapted for. Note that the bandwidth on which the FP acts as a narrow-band filter is limited (on the left and right) due to total transmission of the mirrors of the FP that one could already observe in figure 4.21.

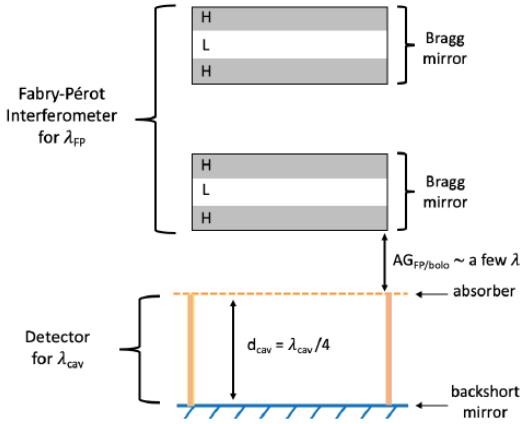

FIGURE 4.23: Coupling of the FPI with a simplified detector. The FPI is based on Bragg mirrors as described previously while the detector is represented by an absorber above a quarter-wave cavity closed by a backshort mirror. The resonant wavelengths λ_{FP} and λ_{cav} of each individual system are not necessarily equal. The bolometer and the FPI are separated by an order of wavelength.

S. Bounissou's PhD thesis (2019)